ELSEVIER

Fisheries Research 47 (2000) 201–214

FISHERIES RESEARCH

www.elsevier.com/locate/fishres

Measurements of three-dimensional fish school velocities with an acoustic Doppler current profiler

David A. Demer[a,*], Manuel Barange[b], Alan J. Boyd[b]

[a]Southwest Fisheries Science Center, PO Box 271, La Jolla, CA 92038, USA
[b]Sea Fisheries Research Institute, Private Bag X2, 8012 Rogge Bay, Capetown, South Africa

Abstract

A method was developed to measure horizontal and vertical velocities of acoustic scattering layers using a multi-beam acoustic Doppler current profiler (ADCP). To determine three orthogonal velocity vectors (east, north, and vertical), it was required that the ADCP beams simultaneously insonified a coherently moving fish school in the same depth bin. Velocity vectors that satisfied these conditions were extracted from individual ping velocity estimates and ensemble-averaged to determine the average speeds and directions of fish aggregations. The results indicate that the ADCP can be a useful tool for observing fish and possibly zooplankton behavior in certain situations. Preliminary investigations include the quantification of horizontal and vertical migration patterns and possible vessel avoidance reaction of large schools of sardine in False Bay, South Africa. The method can be enhanced by refining equipment parameters such as water mode and depth bin length, correcting for rotational motion of the ADCP platform, and possibly by directly processing the radial velocity components from each beam. © 2000 Elsevier Science B.V. All rights reserved.

Keywords: Fish; Three-dimensional; Velocities; Doppler; ADCP; Behavior

1. Introduction

Attempts to use the Doppler effect for the study of fish behavior have been made with varying degrees of success for at least three decades (Hester, 1967). The frequency shift in a transmitted signal caused by movement of fish schools relative to a single acoustic projector (f_D) was used to study radial swimming velocities relative to the water as a function of time ($v_r(t)$):

$$f_D = 2f\frac{v_r(t)}{c}, \tag{1}$$

where f is the frequency of the transmitted signal and c is the speed of sound (Holliday, 1972; Vent et al., 1976). Using similar methods, avoidance behavior of fish in reaction to a survey vessel has also been observed (Olsen and Lovik, 1982). In the present study, a multi-beam acoustic Doppler current profiler (ADCP) was employed (RD Instruments, 1993a) to measure the average horizontal and vertical velocity components of fish schools over a period of time. This work expands upon previous studies by: (1) directly and simultaneously measuring three orthogonal velo-

* Corresponding author. Present address: Southwest Fisheries Science Center, 8604 La Jolla Shores Dr., La Jolla, CA 92037, USA. Tel.: +1-619-546-5603; fax: +1-619-546-5608.
E-mail address: ddemer@ucsd.edu (D.A. Demer)

PII: S0165-7836(00)00170-3

city components (i.e. north, east, and vertical) as opposed to a single radial velocity; (2) referencing the fish velocity vectors to earth, water, or instrument coordinates; and (3) utilizing downwardly projecting beams.

Holliday (1974, 1977) measured the frequency distribution of energy in direct path echoes from three schools of pelagic fish at horizontal distances up to 1200 m. One-half-second 30 kHz pulses were transmitted every 100 s, and a Doppler spread of 30–70 Hz was measured. The target dimensions were 40–120 m along the beam-axis of the sonar. For side-aspect echoes, these frequency shifts were related to fish swimming speed, length, tail-beat amplitude, and tail-beat frequency. For near head- or tail-aspect returns, behavioral swimming characteristics were inferred. A 11 kHz sonar was also deployed from the drifting ship to simultaneously track the schools for 1 h or more. This technique allowed for necessary ensemble averaging of the Doppler data (running average of seven successive pings) without catastrophic violations of the requirements of stationarity. Assuming the swimming direction of the fish school was, on the average, parallel to the sonar beam, average swimming speeds ranging from 0.5 to 1.4 m/s were recorded. If the fish velocity vectors were at an angle to the acoustic beam axis (α), a smaller Doppler shift would have resulted:

$$f_D = 2f\frac{v_r(t)}{c}\cos(\alpha). \qquad (2)$$

From the swimming speed profiles, estimates were made of individual fish sizes, short- and long-term energy expenditures, and species.

Vent et al. (1976) used the same 30 kHz sonar as Holliday (1972, 1974, 1977) but with coded-pulse transmissions and a 200–600 m range-gate. The transmit sequence (fourteen 10 ms pulses followed by a 1 s delay and later by a 170 ms pulse) was repeated every 2 s. A crystal oscillator was used to obtain frequency accuracy to ± 0.6 Hz. The signals received from the 170 ms pulses were processed by amplification and bandpass filtering. The signals were then multiplied by a 29.5 kHz signal and the sum frequency was filtered off, leaving a 500 Hz narrowband signal for analysis. The signal was digitized at 2.048 kHz (approximately four samples per cycle). Targets which had a target strength (TS) greater than -20 dB for more than 42 ms were considered. These target signals were transformed with a 1024-point fast Fourier transform (FFT) (about 500 ms). The radial target speeds were referenced to the background volume reverberation at a range just prior to the target. The fish school velocity measurements had a mean of 0, with a standard deviation of 1.2 kn, implying no net motion either towards or away from the vessel. The authors noted a velocity uncertainty (η) in their measurements due to the finite beamwidth of the transducer (10°). For example, if there was a relative velocity between the vessel and fish of about 6 m/s, the uncertainty would have ranged from 0 for targets on the acoustic axis to approximately ± 0.5 m/s for targets insonified at the -3 dB angles (see Eq. (2) and Fig. 1).

Olsen and Lovik (1982) also used a sonar directed at a fixed tilt-angle to measure Doppler shifts in the echoes from fish schools. The frequency, pulse length, repetition rate, and range were approximately 30 kHz, 30 ms, 0.75 pings/s, and 250 m (Olsen, personal communication, 1995). The spectra of 50 successive pings were averaged, and the frequency of the bottom echo signal was used as a reference for each estimate. Velocity estimates were made of herring and cod as a function of the vessel speed. The results indicated that the fish swam away from the passing vessel while descending to greater depths. This avoidance behavior was accentuated with increasing vessel speed but was less evident for deeper fish shoals. Additionally, the fish exhibited an apparent "stimulus adaptation". Assuming a burst swimming speed of 3 kn, the descent angles of these fish were estimated as 25–30° for the herring and 15–20° for the cod.

In contrast to the aforementioned methods for measuring Doppler frequency shifts (i.e. low frequencies, long pulses, narrow bandwidths, and Fourier transforms), increased velocity and range resolution can be achieved using higher frequencies, coded-pulse trains, and autocorrelation detection of the phase shifts in the backscatter signal (Miller and Rochwarger, 1972). The ADCP uses such methods and four beams, each typically oriented 30° off-vertical (Janus configuration), to derive three orthogonal current vectors (RD Instruments, 1993a). Using trigonometric relations, one beam is required to measure each current component (e.g. east, north and vertical), and the fourth beam provides a redundant estimate of the vertical velocity. The difference between the two

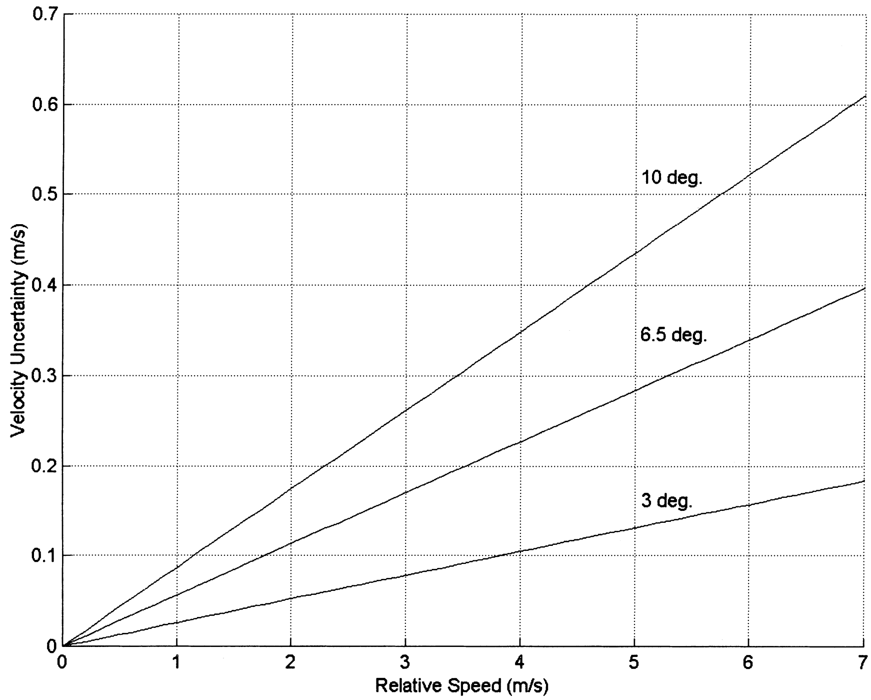

Fig. 1. Doppler velocity measurements have an uncertainty (η) due to finite transducer beamwidths. For transducer beamwidths of 3°, 6.5°, and 10°, the velocity uncertainty (m/s) is determined by $\eta = V_0 \sin(\alpha)$, where V_0 is the relative speed between the target and the vessel and α is the off-axis detection angle (Vent et al., 1976).

estimates of vertical velocity, or error velocity, is used to validate the necessary assumption that the velocity of the scattering layer is horizontally homogeneous at a constant depth, or the same in all four beams (Figs. 2 and 3).

The ADCP measures three-dimensional velocities relative to itself. Referencing the vectors to earth coordinates is subsequently effected by correcting for rotation (pitch and roll) and translation (ship speed and direction). The orientations of the transducer beams are surveyed during installation into a ship's hull. Later they are dynamically identified with outputs from a gyro-stabilized compass and pitch-and-roll sensor (Trump, 1994). Geographic position and the ship velocity are supplied to the ADCP from a global positioning system receiver (GPS). However, due to the practical accuracy limits imposed by "selective availability" (approximately 100 m), the vessel velocity may be more accurately derived from the ADCP data itself. In "bottom reference mode", the ship velocity is measured via bottom tracking, concurrent with the water velocity estimates.

Despite its advantages, the ADCP broadband-processing scheme has multiple constraints. Due to pattern repetition in the transmitted pulse train, a phase shift measured by the autocorrelation method can correspond to velocities in more than one velocity range. The maximum velocity in the lowest velocity range is termed the ambiguity velocity.

Adjustable pulse lengths and range-gating are used to derive velocity estimates for up to 128 depth cells. Increasing the pulse duration (τ) causes a decrease in the bandwidth (BW) of the transmitted signal (BW=1/τ), which in turn reduces the uncertainty in the estimates of Doppler frequencies and velocities. Also, averaging the individual velocity estimates within a depth cell reduces both the effects of aliasing and the variance of the measurements. The length of the pulse and the depth cell are typically chosen to be the same. Thus, the random error of velocity measurements varies inversely with the size of the depth cell. For

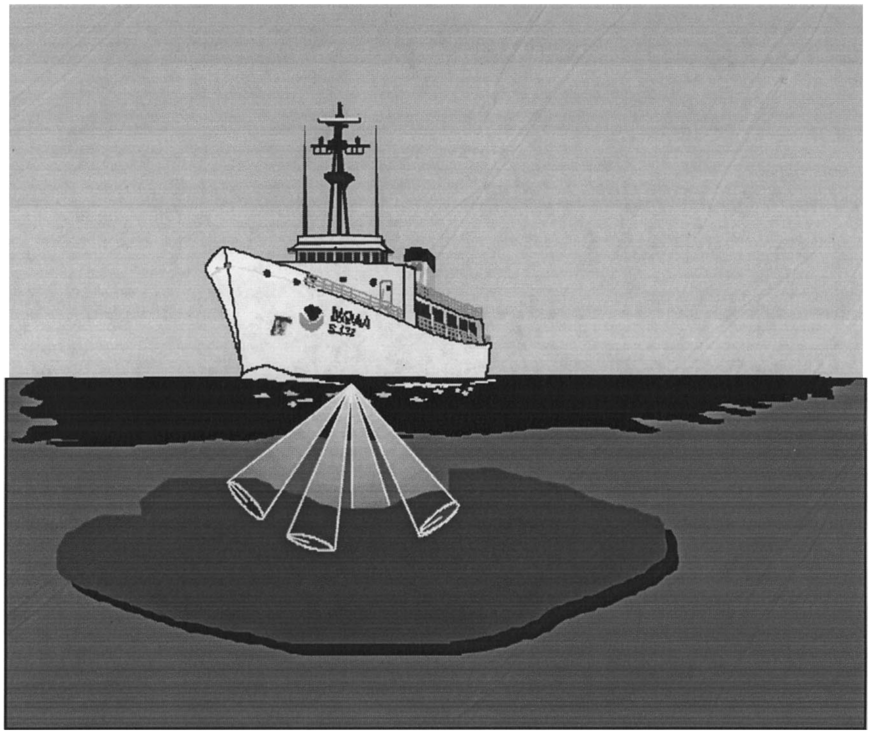

Fig. 2. Measurement of three-dimensional velocities of fish or zooplankton aggregations requires that at least three of the four ADCP beams intersect the acoustic scattering layer. Moreover, the scattering layer must be moving homogeneously so that that each of the beams are recording velocity components of the school's coherent motion.

example, if a 150 kHz Broadband ADCP is configured with the normal water profiling mode, the standard deviation of the horizontal velocity component relative to the instrument is approximately 10, 4, and 2 cm/s for 2, 3, and 8 m depth cells, respectively (RD Instruments, 1993a). To reduce the standard deviation of individual ping velocity estimates by a factor of $1/N^{1/2}$, data from numerous pings (N) are normally averaged (ensemble averaging). Measurement bias is typically 0.2% of the measured velocity ± 2 cm/s (RD Instruments, 1993a).

Further bias can result from acoustic backscattering from fish (Freitag et al., 1992). Therefore, the ADCP firmware includes a fish rejection algorithm that screens the velocity data for fish (Freitag et al., 1993). This algorithm is based upon the maximum difference between echo intensity readings among the four profiling beams. If a threshold value is exceeded, the ADCP rejects the velocity data on a cell-by-cell basis. If fish are detected in only one beam, then the data from that beam, for that cell, are discarded. If fish are detected in more than one beam, the data from all four beams are discarded for that cell.

Clearly, the ADCP is not designed to study the three-dimensional velocities of fish. Therefore, to use the instrument for extracting fish behavioral information, one must: (1) modify the operating parameters and data processing routines; (2) choose survey situations when the ADCP beams simultaneously ensonify a coherently moving aggregation of fish (e.g. pelagic fish layers at night); and (3) measure velocities of nearby water void of fish, but having the same currents as that of the school's environment (e.g. by moving just outside the fish aggregation or waiting for the fish to form shoals after sunrise). This paper summarizes a feasibility study regarding the usage of an ADCP for measuring horizontal and vertical velocities of fish schools.

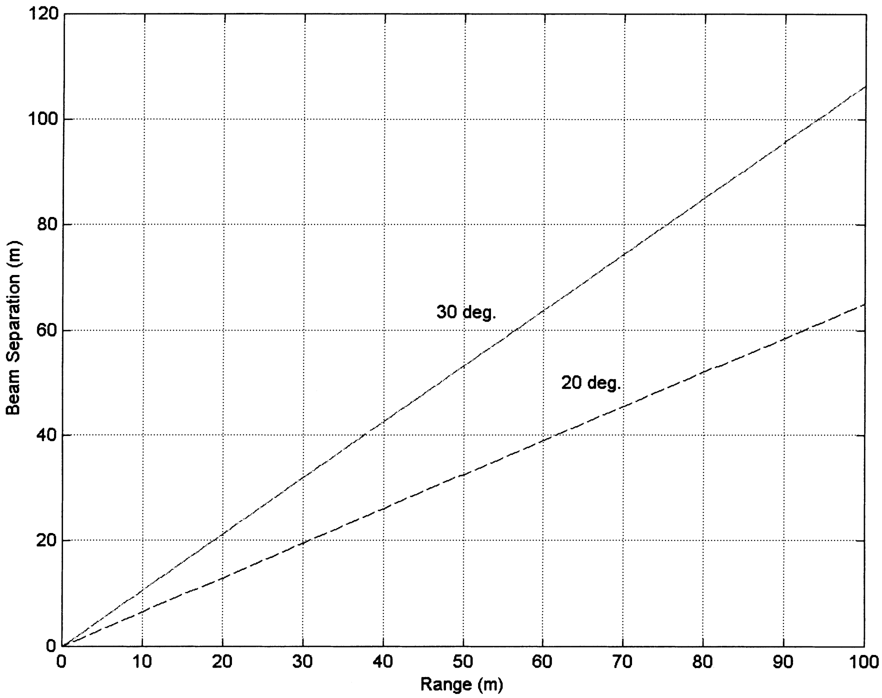

Fig. 3. Beam separation versus range for ADCP transducer configurations (determined for closest -3 dB points of transducers with 3° beamwidths). This separation determines the minimum horizontal dimension of a fish school for it to be simultaneously insonified within the half-power points of two transducer beams. Note that the 20° configuration reduces the requisite school dimension by about 40% and therefore may be a better choice for ADCP measurements of fish velocities. The tradeoff, however, is that the smaller angular separation between transducers has the effect of decreasing measurement precision by a factor of about 1.5 (RD Instruments, 1989).

2. Methods

A 153 kHz broadband ADCP, mounted "down-looking" in the hull of the R/V Dr. Fridtjof Nansen, was deployed in False Bay, South Africa from 11 to 16 October 1995. The four transducers had nominal beamwidths of 3° and were mounted in the 30° Janus configuration. The ADCP was operated with firmware version 5.27 (RD Instruments, 1993a). System configuration and data post-processing were conducted with Broadband Transect software version 2.70 (RD Instruments, 1993b) and custom programs written in version 4.2c of Matlab (The Mathworks, 1992).

The ADCP data were collected at different times with 2, 4, or 8 m depth bins over ranges which allowed a constant 1 s ping repetition rate (25, 20, and 15 bins, respectively). The blank after transmit was 4 m and the maximum bottom depth was adjusted between 60 and 80 m, as appropriate. Favorable weather conditions and the ship's retractable centerboard provided sufficient stability so that the pitch and roll compensation was disabled (Table 1). Most importantly, the fish rejection algorithm was disabled (control setting WA255).

The broadband ADCP can be set to operate with one of the five different water velocity profiling modes. Each mode uses a different pulse sequence and processing algorithm resulting in different ambiguity velocities and standard deviations of the velocity estimates. For these experiments, water mode 1 was selected. This mode uses a set of pulses with a short lag and has a default ambiguity velocity of about ±10 m/s. Mode 1 was initially selected because it avoids ambiguity-resolving errors when there are sudden changes in velocity — for instance when swimming fish are encountered. The tradeoff is a velocity standard deviation which is at least twice

Table 1
Direct command settings used to configure the broadband ADCP[a]

WS400[b]	Depth cell size; set to 2, 4, or 8 m depending on layer thickness
WF400	Blank after transmit; set to 4 m
BX800[b]	Bottom tracking maximum tracking depth; set to 80 m
WN018[b]	Number of depth cells; set to 30, 20, or 18 depending on depth cell size
WD111100000	ADCP data out telegram
WP00001[b]	Pings per ensemble; set to 1
BP001	Bottom tracking pings per ensemble; set to 1
WM1[b]	Water profiling mode; set to 1
TP000100[b]	Time between ping groups; set to 1 s
EP0000	Pitch (tilt 1); set to 0.000°
ER0000	Roll (tilt 2); set to 0.000°
EZ1120001	Sensor source
BE5000	Bottom tracking error velocity maximum; set to 5 m/s
BA20	Bottom tracking evaluation amplitude minimum; set to 20 counts
BC200	Bottom tracking correlation magnitude minimum; set to 200 counts
WA255[b]	False-target threshold maximum; disabled with setting of 255

[a] Single-ping ensemble data was logged as "Raw", "Processed", and "Navigation" data files. The "Processed" files were subsequently converted to ASCII and post-processed using Matlab programs. The "Raw" and "Navigation" files were stored for additional analyses and program development (see RD Instruments, 1993b for detailed data descriptions).

[b] Particular attention paid.

as high as the normal profiling mode (water mode 4; RD Instruments, 1993a).

Individual ping data were recorded and post-processed using the following fish velocity detection algorithm:

1. In an area void of fish, an average background echo intensity profile was recorded for each of the four ADCP beams.
2. In the same survey segment void of fish, the individual-ping currents estimates were ensemble-averaged (see Appendix A).
3. In a nearby area with fish, the intensity data from each of the four beams were compared to the corresponding four background intensity profiles.
4. In the event that all four of the bin intensities exceeded the background values by a set threshold margin, the velocity estimates from that depth bin were judged to be caused by fish and were saved to a file.
5. The individual-ping fish velocity estimates were ensemble-averaged for a survey segment that corresponded to relatively uniform environmental and biological conditions (see Appendix A).
6. The background currents were compared to the average fish velocity estimates to achieve values referenced to the water.

3. Results

Operating with the parameters described above and in Table 1, the ADCP was used to collect fish school velocity data during two trial periods.

Trial 1. On 11 October 1995, from 20:32 to 21:50 GMT (night-time), the ship was positioned over a continuous, high-density fish layer extending from 20 to 30 m depth (Fig. 4). The ADCP depth cell size was set to 2 m. A 5 min segment of this trial was relatively free from fish scatterers and was therefore used to compile a background intensity profile for the four beams (Fig. 5). Distributions of velocity data were created for cells that passed a somewhat arbitrary 5 dB threshold margin (Fig. 6). Increasing the threshold margin to 10 dB had the effect of substantially decreasing the number of fish velocity measurements. The mean ($\bar{x}$), standard deviation (σ), and number of observations (N) were calculated for each distribution (Table 2).

The velocity data (cm/s) were corrected for the ship's speed and direction of 1.7 kn (σ=0.3) and 130° (σ=17), respectively. Note that the mean horizontal and vertical fish velocities were approximately +28 and −3 cm/s different than the background current velocities in the fish depth range (18–32 m). However, due to the sample size and incoherent

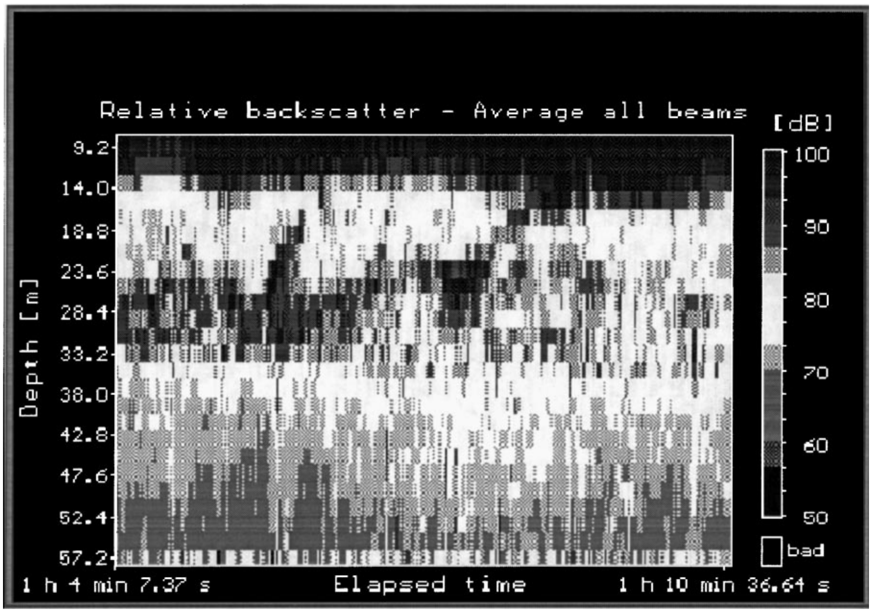

Fig. 4. Trial 1 average intensity echogram showing continuous fish scattering layer from approximately 18 to 32 m depth at night.

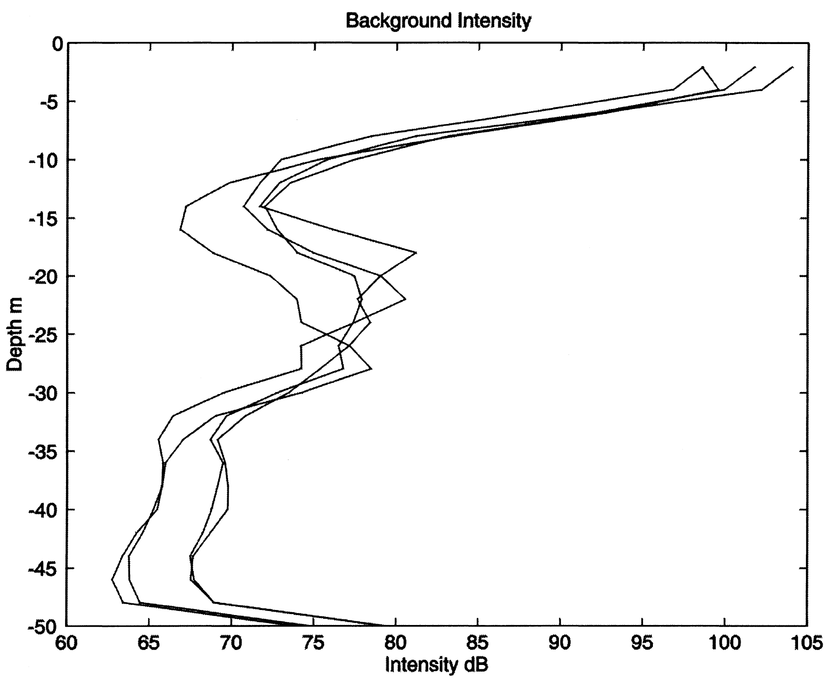

Fig. 5. Trial 1 background intensity profile. Despite efforts to choose a survey portion void of fish but in an area nearby the fish, some scatter from fish has clearly contaminated the background intensity profile (20–40 m). Since subsequent fish echoes (resolved by individual pings, beams, and cells) were identified by their intensities relative to the background profile, an impure background intensity profile will unnecessarily reduce the number of fish velocity measurements that exceed the threshold.

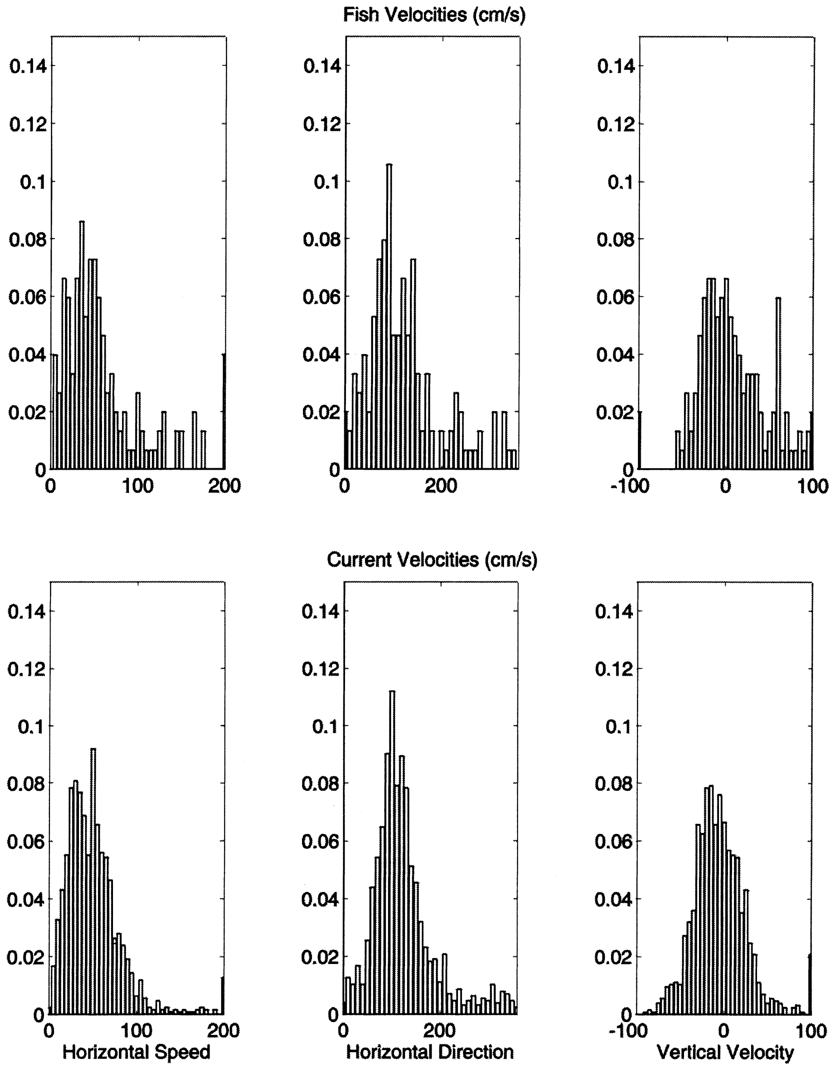

Fig. 6. Trial 1 histograms for fish and current velocity estimates. Histograms are for fish-to-background thresholds of 5 dB.

movements of individual fish, the standard deviations of the fish speed distributions were significantly larger than those for the ambient current.

Trial 2. On 13 October 1995, from 14:23 to 16:01 (day-time), the ship traveled south at a speed of approximately 3 kn in an area of numerous dense fish schools. The discrete schools resided at various depths from the surface to the bottom (Fig. 7). The ADCP depth cell size was set to 2 m. A 5 min segment of this trial was free from fish scatterers and was therefore used to compile a background intensity profile for the four beams (Fig. 8). Distributions of velocity data were created for cells that passed a 5 dB threshold margin (Fig. 9). The mean, standard deviation, and number of observations were calculated for each distribution (Table 3).

The velocity data were corrected for the ship's speed and direction of 1.26 kn (σ=0.6) and 178.5° (σ=27.6), respectively. Note that the mean horizontal and vertical fish velocities were approximately +45 and +11 cm/s different than the background current velocities in the fish depth range (15–50 m). Again,

Table 2
Summary statistics for Trial 1 and corresponding to Fig. 6[a]

Start date	11/10/1995	Start time	20:32Z	End date	11/10/1995	End time	21:23Z		
Start latitude	34.286S	Start longitude	18.672W	End latitude	34.268S	End longitude	18.689W		
Minimum depth (m)		18		Maximum depth (m)		38			
	Single-ping statistics								
	Horizontal speed (cm/s)		Horizontal direction		Vertical velocity (cm/s)		N		
	$\bar{x}$	σ	$\bar{x}$	σ	$\bar{x}$	σ			
Fish (>5 dB)	81	148	122	78	0	95	151		
Current	53	47	125	66	−3	42	1250		
	Vector averages								
	Speed (cm/s)		Azimuth (°)			Elevation (°)			
Fish (>5 dB)	15		279			0			
Current	4		311			−50			

[a] The velocity data (cm/s) were corrected for the ship's speed and direction of 1.7 kn (σ=0.3) and 130° (σ=17), respectively. Note that the mean horizontal and vertical fish velocities were approximately +28 and −3 cm/s different than the background current velocities in the fish depth range (18–32 m). However, due to sample size, the standard deviations of the fish speed distributions were significantly larger than those for the ambient current.

due to sample size and incoherent movements of individual scatterers, the standard deviations of each fish speed distribution were larger than those for the current.

Four additional case studies from False Bay, South Africa, are summarized in Table 4. Collectively, these studies suggest that it is possible to successfully repeat the initial trials using a narrowband ADCP and to quantify animal behaviors such as swimming into the prevailing current, while filter-feeding or diving in front of trawling nets as an avoidance reaction.

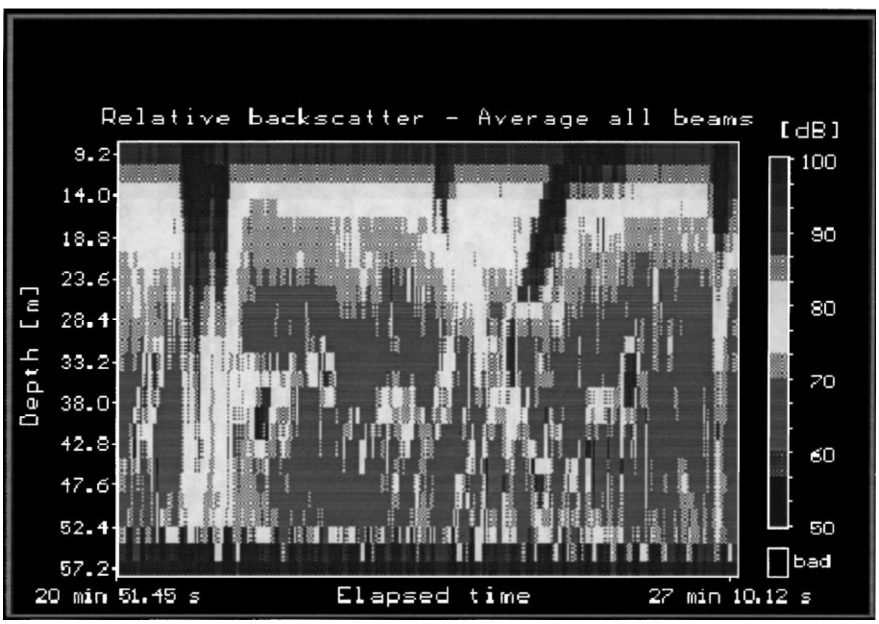

Fig. 7. Trial 2 average intensity echogram showing discrete dense fish schools distributed from the surface to the bottom during daylight.

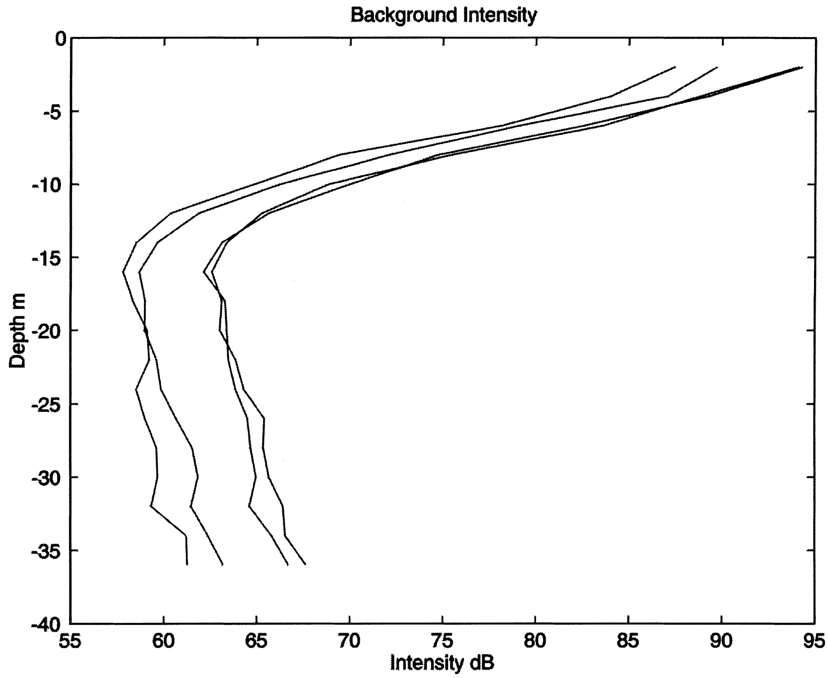

Fig. 8. Trial 2 background intensity profile. Fish echoes were identified from the intensities of individual pings, beams, and cells. Clear water between the fish schools easily provided a relevant background intensity profile uncontaminated by fish echoes.

4. Discussion

In summary, this study indicates that the ADCP can be used to measure three-dimensional velocities of fish or zooplankton aggregations relative to the earth, the water, or the ADCP in certain situations:

1. The scattering layer must be large enough to backscatter sound from at least three of the four transducers in the ADCP array (four if analyzing "Processed data", three if using "Raw data"). Smaller angles in the Janus configuration (e.g. transducers aiming 20° off-vertical opposed to the standard 30° configuration) will reduce the requisite scattering layer dimensions (see Fig. 3). Unfortunately, relative to the 30° configuration, the random error of the horizontal velocity components is increased by about 1.5 in the 20° configuration (RD Instruments, 1989).
2. The scattering layer must be moving homogeneously at a given depth. For example, layers of fish or zooplankton moving on- or off-shore or vertically migrating. However, incoherent movements of the individual scatterers (i.e. fish avoiding the research vessel by moving downward under the ship and horizontally away from both sides of the ship) will void a requisite assumption for measuring three-dimensional velocities and induce a high error velocity.
3. The velocities of the collective scattering layer must exceed the ADCP measurement precision. Provided that the noise is random and the aggregation is behaving similarly through the measurement duration (both in time and space), ensemble averaging of the individual ping data will increase the single-ping measurement precision.
4. To reference the three-dimensional fish velocities to anything other than the ADCP, movements of both the ship (and ADCP) and the relevant background currents must be adequately characterized. Accurate measurement of the background currents may be facilitated by the shoaling behavior of pelagic fish which can form a moderately dense, but uniform, scattering layer at night, and break up into discrete shoals amongst

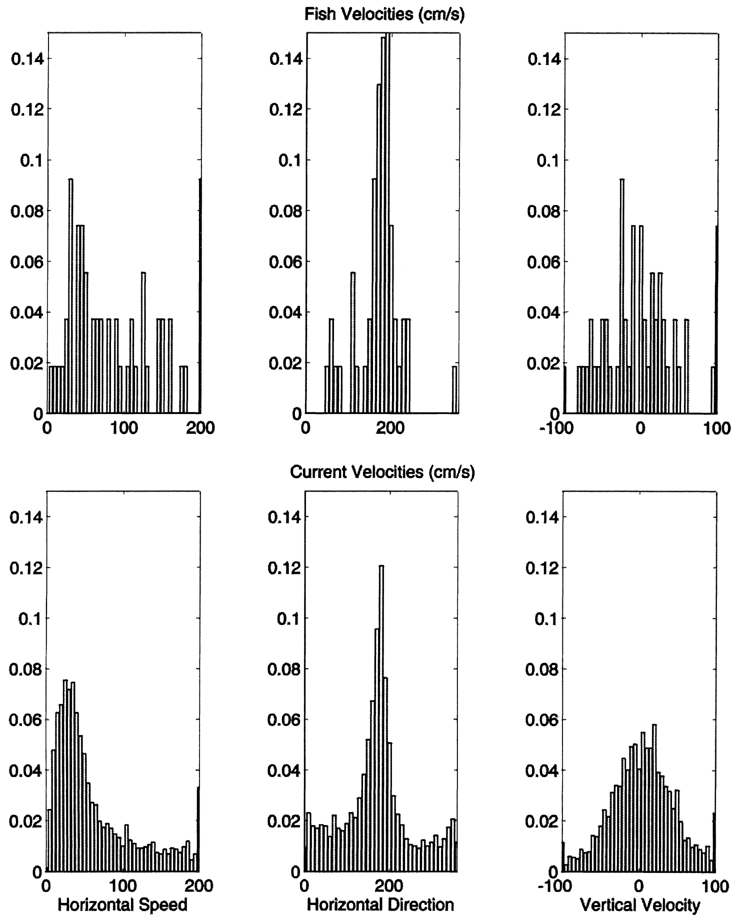

Fig. 9. Trial 2 histograms for fish and current velocity estimates. Histograms are for fish-to-background thresholds of 5 dB.

Table 3
Summary statistics for Trial 2 and corresponding to Fig. 9[a]

Start date	13/10/1995	Start time	14:28Z	End date	13/10/1995	End time	15:57Z
Minimum depth (m)		15		Maximum depth (m)		50	
	Single-ping statistics						
	Horizontal speed (cm/s)		Horizontal direction		Vertical velocity (cm/s)		*N*
	$\bar{x}$	σ	$\bar{x}$	σ	$\bar{x}$	σ	
Fish (>5 dB)	112	144	171	51	17	107	54
Current	67	73	171	81	6	47	2172
	Vector averages						
	Speed (cm/s)		Azimuth (°)			Elevation (°)	
Fish (>5 dB)	28		312			39	
Current	6		8			77	

[a] The velocity data were corrected for the ship's speed and direction of 1.26 kn (σ=0.6) and 178.5° (σ=27.6), respectively. Note that the mean horizontal and vertical fish velocities were approximately +45 and +11 cm/s different than the background current velocities in the fish depth range (15–50 m). Again, due to sample size and incoherent movements of individual scatterers within the layer, the standard deviations of each fish speed distribution were larger than those for the current.

Table 4
Four additional case studies of fish velocities from False Bay, South Africa[a]

Case	Date	Time (GMT)	Position		Activity	Ship's speed (knots)	Ship's heading (°)	Bottom depth (m)	Fish depth (m)	Mean caudal length (cm)
			Latitude	Longitude						
1	14/11/1995	1753	34 18	49.9 35.7	Trawling	3–4	142	200	30–40	15.9
		Speed (cm/s)			Horizontal direction (°)			Elevation (°)		
Current		4			8			60		
Fish		5			6			−83		
Observation. Possible avoidance; round-herring diving in front of the net										
2	15/11/1995	0058	34 18	15.2 40.6	Trawling	3–4	207	56	15–25	11.8
		Speed (cm/s)			Horizontal direction (°)			Elevation (°)		
Current		7			5			−56		
Fish		15			173			−66		
Observation. Filter-feeding sardines moving against current										
3	16/11/1995	1005	34 18	52.8 53.4	Trawling	3–4	200	112	15–30	13
		Speed (cm/s)			Horizontal direction (°)			Elevation (°)		
Current		12			131			−12		
Fish		15			10			7		
Observation. Filter-feeding sardines moving against current										
4	2/12/1996	0253	34 19	25.7 01.7	Trawling	3–4	99	51	15–25	–
		Speed (cm/s)			Horizontal direction (°)			Elevation (°)		
Current		−2			214			60		
Fish		12			59			−85		
Observation. Fish moving against the current and diving										

[a] The data were collected from the FRS Africana, which is equipped with an RD Instruments 153 kHz narrowband ADCP. The ADCP was operating with firmware version 16.26 (without a fish rejection algorithm; direct command CF99 turns off fish rejection algorithm in narrowband firmware version 17.10), and Transect software version 1.80. Results indicate that both the broadband and narrowband ADCP instruments may be useful tools to study fish behaviors such as feeding strategies and avoidance behavior.

patches of open water at daybreak (Barange and Hampton, 1997). These actions could allow the measurement and comparison of water and fish velocities at the same site only an hour or two apart.

5. Conclusion

All six applications of this method for measuring fish velocities with an ADCP have provided indication of fish behaviors that could not have been observed otherwise. In particular, the authors are unaware of references to other methods that have demonstrated fish swimming at the same speed, but opposite direction to the prevailing current. Notwithstanding these encouraging results, these experiments should only be considered as an indication of the potential for further application of this method, possibly with more refined equipment settings and improved data processing algorithms.

Future experiments should be conducted with different water modes in order to optimize the compromise between the ambiguity velocity and the velocity standard deviation. Depth bins should be optimized to minimize the velocity standard deviation while maintaining an acceptable range resolution. If the bin width is too large, fish velocities will be averaged with currents in water void of fish. Tests should be conducted to determine the practical utility of using tilt sensors for pitch-and-roll compensation of the data. Compensation for rotational movements should reduce the uncertainty of the velocity measurements made during bad weather conditions, especially the vertical velocity component. Finally, if fish in schools are not exhibiting coherent movements, the Doppler data from individual beams could be scrutinized and processed independently to observe radial velocities of fish in four directions. This would require processing of the "Raw" data telegram (see RD Instruments, 1993b for data formats). However, conditions to obtain these uni-dimensional velocities should be encountered more frequently, and the results may be adequate for many behavioral studies.

Acknowledgements

This research was conducted as part of a cooperative research project with the Institute of Marine Research (IMT), Bergen, Norway; the Sea Fisheries Research Institute (SFRI), Cape Town, South Africa; the University of Tromso (UT), Tromso, Norway; ORSTROM, Montpellier, France; and the Southwest Fisheries Science Center, La Jolla, USA. Special thanks regarding this study go to Ole Misund, Tore Stroemme, and Oddgeir Alvheim of IMR, Ian Hampton of SFRI, and Kjell Olsen of UT.

Appendix A. Equations for vector averaging the individual ping velocity estimates

Ping number	n
Number of pings in average	N
Single-ping vertical velocity	v_{v_n}
Single-ping horizontal speed	s_{h_n}
Single-ping horizontal direction	θ_n

Average the velocity vectors while converting from cylindrical to rectangular coordinates

$$\text{Mean vertical velocity}: \quad \bar{v}_{\mathrm{v}} = \frac{\sum_{n=1}^{N} v_{\mathrm{v}_n}}{N}.$$

$$\text{Mean east velocity}: \quad \bar{v}_{\mathrm{e}} = \frac{\sum_{n=1}^{N} s_{\mathrm{h}_n} \sin(\theta_n)}{N}.$$

$$\text{Mean north velocity}: \quad \bar{v}_{\mathrm{n}} = \frac{\sum_{n=1}^{N} s_{\mathrm{h}_n} \cos(\theta_n)}{N}.$$

$$\text{Mean horizontal speed}: \quad \bar{s}_{\mathrm{h}} = \sqrt{\bar{v}_{\mathrm{e}}^2 + \bar{v}_{\mathrm{n}}^2}.$$

Convert to spherical coordinates

$$\text{Mean speed}: \quad \bar{s}_{\mathrm{t}} = \sqrt{\bar{v}_{\mathrm{v}}^2 + \bar{v}_{\mathrm{e}}^2 + \bar{v}_{\mathrm{n}}^2}.$$

Mean horizontal direction:

$$\bar{\theta} = \begin{cases} \tan^{-1}(\bar{v}_{\mathrm{e}}/\bar{v}_{\mathrm{n}}) & (\bar{v}_{\mathrm{n}} \geq 0 \text{ and } \bar{v}_{\mathrm{e}} \geq 0), \\ 180^\circ + \tan^{-1}(\bar{v}_{\mathrm{e}}/\bar{v}_{\mathrm{n}}) & (\bar{v}_{\mathrm{n}} < 0), \\ 360^\circ + \tan^{-1}(\bar{v}_{\mathrm{e}}/\bar{v}_{\mathrm{n}}) & (\bar{v}_{\mathrm{n}} \geq 0 \text{ and } \bar{v}_{\mathrm{e}} < 0). \end{cases}$$

Mean elevation:

$$\bar{\phi} = \begin{cases} \tan^{-1}(\bar{v}_{\mathrm{v}}/\bar{s}_{\mathrm{h}}) & (\bar{v}_{\mathrm{v}} \geq 0 \text{ and } \bar{s}_{\mathrm{h}} \geq 0), \\ \tan^{-1}(\bar{s}_{\mathrm{h}}/\bar{v}_{\mathrm{v}}) - 90^\circ & (\bar{v}_{\mathrm{v}} < 0 \text{ and } \bar{s}_{\mathrm{h}} < 0), \\ -(\tan^{-1}(\bar{s}_{\mathrm{h}}/\bar{v}_{\mathrm{v}}) + 90^\circ) & (\bar{v}_{\mathrm{v}} < 0 \text{ and } \bar{s}_{\mathrm{h}} \geq 0), \\ -\tan^{-1}(\bar{v}_{\mathrm{v}}/\bar{s}_{\mathrm{h}}) & (\bar{v}_{\mathrm{v}} \geq 0 \text{ and } \bar{s}_{\mathrm{h}} < 0). \end{cases}$$

References

Barange, M., Hampton, I., 1997. Spatial structure of co-occurring anchovy and sardine populations from acoustic data: implications for survey design. Fish. Oceanogr. 6 (2), 94–108.

Freitag, H.P., McPhaden, M.J., Pullen, P.E., 1992. Fish induced bias in acoustic Doppler current profiler data. Proc. Oceans'92. 1, 712–717.

Freitag, H.P., Plimpton, P.E., McPhaden, M.J., 1993. Evaluation of an ADCP fish-bias rejection algorithm. Proc. Oceans'93. 2, 394–397.

Hester, F.J., 1967. Identification of biological sonar targets from body motion Doppler shifts. In: Tavolga, W.N. (Ed.), Symposium on Marine Bioacoustics, Vol. 2. Pergamon Press, New York, pp. 59–74.

Holliday, D.V., 1972. Resonance and Doppler structure in echoes from pelagic fish schools. Ph.D. Thesis. University of California Press, San Diego, CA.

Holliday, D.V., 1974. Doppler structure in echoes from schools of pelagic fish. J. Acoust. Soc. Am. 55 (6), 1313–1322.

Holliday, D.V., 1977. Two applications of the Doppler effect in the study of fish schools. ICES J. Mar. Sci. 170, 21–30.

The Mathworks, 1992. Matlab Reference Guide: High-Performance Numeric Computation and Visualization Software, Natick, MA, USA.

Miller, K.S., Rochwarger, M.M., 1972. A covariance approach to spectral moment estimation. IEEE Trans. Inform. Theory. 18 (5), 588–596.

Olsen, K., Lovik, A., 1982. Observed fish reactions to a surveying vessel with special reference to herring, cod, capelin and polar cod. Symp. Fish. Acoust., Bergen, Norway. 48, 21–24.

RD Instruments, 1989. Acoustic Doppler Current Profilers. RD Instruments, San Diego, CA, 37 pp.

RD Instruments, 1993a, Direct-reading Broadband Acoustic Doppler Current Profiler Technical Manual. RD Instruments, San Diego, CA.

RD Instruments, 1993b. User's manual for the RD Instruments Transect Program (for use with Broadband ADCP). RD Instruments, San Diego, CA.

Trump, C.L., 1994. Three practical hints on using vessel mounted ADCPs. MTS J. 33 (2), 28–35.

Vent, R.J., Davies, I.E., Townsend, R.W., Brown, J.C., 1976. Fish school target strength and Doppler measurements, Southwest Fisheries Center Admin. Report No. LJ-76-15, La Jolla, CA, 32 pp.